# A Blazar-Like Radio Flare in Mrk 231

Cormac Reynolds[1], Brian Punsly[2], Christopher P. O'Dea[3], Natasha Hurley-Walker[1]

## ABSTRACT

Radio monitoring of the broad absorption line quasar (BALQSO) Mrk 231 from 13.9 GHz to 17.6 GHz detected a strong flat spectrum flare. Even though BALQSOs are typically weak radio sources, the 17.6 GHz flux density doubled in $\approx$ 150 days, from $\approx$ 135 mJy to $\approx$ 270 mJy. It is demonstrated that the elapsed rise time in the quasar rest frame and the relative magnitude of the flare is typical of some of the stronger flares in blazars that are usually associated with the ejection of discrete components on parsec scales. The decay of a similar flare was found in a previous monitoring campaign at 22 GHz. We conclude that these flares are not rare. The implication is that Mrk 231 seems to be a quasar in which the physical mechanism that produces the BAL wind is in tension with the emergence of a fledgling blazar.

*Subject headings:* quasars: absorption lines — galaxies: jets — quasars: general — accretion, accretion disks — black hole physics

## 1. Introduction

One of the main mysteries of the quasar phenomenon is the associated powerful outflows that come in a variety of forms. These outflows can be manifest as extremely energetic relativistic jets $>$ 100 kpc in extent or massive broad absorption line (BAL) winds. Furthermore, the existence of large scale jets and BAL winds are almost mutually exclusive. The propensity for suppressed large scale emission increases strongly with BALnicity index (Becker et al. 2000, 2001)[1]. From Very Long Baseline Array (VLBA) studies of the

[1]ICRAR-Curtin University, GPO Box U1987, Perth, Western Australia, 6102, Australia

[2]1415 Granvia Altamira, Palos Verdes Estates CA, USA 90274 and ICRANet, Piazza della Repubblica 10 Pescara 65100, Italy, brian.punsly1@verizon.net or brian.punsly@comdev-usa.com

[3]Laboratory for Multiwavelength Astrophysics, School of Physics and Astronomy, Rochester Institute of Technology, 54 Lomb Memorial Drive,Rochester, NY 14623

[1]We use the original definition of a BAL as UV absorbing gas that is blue shifted at least 5,000 km/s relative to the QSO rest frame and displaying a spread in velocity of at least 2,000 km $s^{-1}$, (Weymann et al.

BAL quasar (BALQSO) Mrk 231 in Reynolds et al. (2009) and other radio quiet quasar studies, it has become evident that radio quiet active galactic nuclei (AGN) can have relativistic outflows with significant kinetic luminosity, but possibly only for short periods of time (Brunthaler et al 2000; Blundell et al 2003). So this raises the question what is it that makes some sources radio quiet and others radio loud? Does the BAL wind inhibit the efficacy of jet initiation or does it simply limit the ability of a jet to propagate to large distances, or both? At a redshift of $z = 0.042$, Mrk 231 is one of the nearest radio quiet quasars to earth. The radio core is perhaps the brightest of any radio quiet quasar (and certainly the brightest BALQSO core) at high frequency (22 and 43 GHz). Studying the radio core at high frequency can provide vital clues to the origin of both the large scale radio jets and the BAL winds in AGN. Thusly motivated, the authors have embarked on a program of high frequency VLBA observations (Reynolds et al. 2009) and long term high frequency, densely time sampled, low resolution radio monitoring. We report our first four years of radio monitoring results here.

The paper is organized as follows. Section 2 will describe previous evidence of the blazar-like nature of Mrk 231. This is the motivation for expected dramatic behavior in the high frequency light curve. The next section describes the observational details of our monitoring. In Section 4, we compare our most recent epoch of monitoring to typical strong blazar flares. Throughout this paper, we adopt the following cosmological parameters: $H_0$=71 km s$^{-1}$ Mpc$^{-1}$, $\Omega_\Lambda = 0.73$ and $\Omega_m = 0.27$.

## 2. Previous Observed Blazar-Like Behavior

The most striking finding in our summary of the VLBA observation in Reynolds et al. (2009) was the strong 22 GHz flare that emerged from the core between epochs 2006.07 and 2006.32 ($> 150\%$ increase in less than 3 months). All attempts in Reynolds et al. (2009) to model the high frequency peak of the spectral turnover, 19.5 GHz, in combination with the steep spectral index[2] above 22 GHz ($\alpha \approx 2$) indicate that the flare is synchrotron self-

1991). Note that this definition specifically excludes the so-called "mini-BALQSOs," with the BALNicity index = 0 (Weymann 1997). This is desirable since the DR5 statistical analysis of Zhang et al. (2010) indicate that these types of sources (mini-BALQSOs have a large overlap in definition with the intermediate width absorption line sources of Zhang et al. (2010)) tend to resemble non-BALQSOs more than BALQSOs in many spectral properties. Mini-BALQSOs also tend to have much smaller X-ray absorbing columns than BALQSOs (Punsly 2006). Typically, "BALQSO" radio targets are actually mini-BALQSOs since they have larger radio fluxes than bona-fide BALQSOs, e.g. Bruni et al. (2013); Hayashi et al. (2013).

[2]for spectral index we use $S_\nu \propto \nu^{-\alpha}$ throughout.

absorbed and the brightness temperature is $T_B \approx 10^{12}$ K, unless the flux density is Doppler boosted. The Doppler boosted models indicated an intrinsic (rest frame of the plasma) brightness temperature $\gtrsim 10^{11}$ K. The modeling of the flare in Reynolds et al. (2009) also requires that the bulk of the flare emission is from a region on the order of $3 \times 10^{16}$ cm.

There is strong corroboration in the literature of this blazar-like behavior. A $134 \pm 38$ mJy flux density variation in 1 day at 22.2 GHz was reported in McCutcheon and Gregory (1978). This can be seen in Figure 1. Using the methods of Ghosh and Punsly (2007), the time variability brightness temperature was found in Reynolds et al. (2009) to be $T_B = (12.4 \pm 3.5) \times 10^{12}$ K. If the brightness temperature ($T_B$) exceeds $10^{12}$ K, it requires a nearly pole-on orientation and relativistic motion for the jet in order to avoid the "inverse Compton catastrophe" (Marscher et al. 1979). This indicates that the line of sight to the jet is restricted kinematically to $\theta_{max} < (25.6^\circ)^{+3.2^\circ}_{-2.2^\circ}$ (Reynolds et al. 2009).

## 3. The Radio Observations

### 3.1. Observations and Calibration

The program utilized long term monitoring with the VLA (Very Large Array) and EVLA (Expanded Very Large Array) at 22 GHz and AMI (Arcminute Microkelvin Imager; Zwart et al. 2008) at 13.5 – 18 GHz [3]. These data are plotted in Figure 1 along with historical data both from the literature (McCutcheon and Gregory 1978; Edelson 1987; Ulvestad et al 1999a,b; Reynolds et al. 2009) and from the VLA public archive (project codes AB783, AN030, AU015). Both our monitoring data and the data from the VLA archive were calibrated using NRAO's AIPS package via the ParselTongue interface (Kettenis et al. 2006) in the standard way. 3C 286 served as the primary flux calibrator in all the VLA observations. In our VLA/EVLA monitoring observations (2009 – 2012) we also made use of J1219+4829 as a nearby secondary flux calibrator. Flux density error estimates on Mrk 231 were confirmed by short scans on another VLA calibrator (J1400+6210) located at a similar separation from the secondary calibrator as Mrk 231 and calibrated in an identical fashion to Mrk 231. Both AMI's Large Array and Small Array were used, but the Small Array data

[3]The Arcminute Microkelvin Imager consists of two radio interferometric arrays located in the Mullard Radio Astronomical Observatory, Cambridge, UK (Zwart et al. 2008). Both arrays observe between 13.9 and 18.2 GHz in six frequency channels. The Small Array (AMI-SA) consists of ten 3.6 m diameter dishes with a maximum baseline of 20 m, yielding an angular resolution of $3'$, while the Large Array (AMI-LA) comprises eight 12.6 m diameter dishes with a maximum baseline of 110 m, giving an angular resolution of $0\farcm5$.

are preferred, as explained below. The AMI data were calibrated using the standard AMI pipeline.

### 3.2. Constructing the Historical 20 GHz Lightcurve

Mrk 231 appears to have no significant 20 GHz emission on scales larger than an arcsecond (it appears as a point source to the VLA in all configurations), so the wide range in spatial resolution provided by the various instruments in the historical observations of this source has little effect on the measured flux densities. The exceptions are the VLBI measurements which resolve out some of the larger scale, presumably diffuse, emission. In order to convert the VLBA data in Reynolds et al. (2009) to that which would have been detected with an array containing shorter baselines (such as the VLA), we separate out the steady background components. In 1996.93 the VLA measured $62\pm9$ mJy at 22 GHz and the nuclear double was observed simultaneously with the VLBA to be $\sim 30$ mJy (Ulvestad et al 1999a). We designate this as $S_{\nu=22\mathrm{GHz}}(\mathrm{wide\ field}) \approx 30$ mJy, which must be added to the VLBA measurement flux density to get the total flux density at 22 GHz (i.e., the 2006 data points in Figure 1). The scientific interest here is to detect the flaring core on the background of the quasi steady component. Three separate VLBA observations resolve the nuclear double at 22 GHz (Reynolds et al. 2009). The secondary flux density, $S_{\nu=22\mathrm{GHz}}(\mathrm{secondary})$, is fairly steady ranging from 36 to 43 mJy. Thus, to find the core flux density from the total flux density at any epoch

$$\begin{aligned} S_{\nu=22\mathrm{GHz}}(\mathrm{core}) &= S_{\nu=22\mathrm{GHz}}(\mathrm{total}) - S_{\nu=22\mathrm{GHz}}(\mathrm{secondary}) - S_{\nu=22\mathrm{GHz}}(\mathrm{wide\ field}) \quad (1) \\ &= S_{\nu=22\mathrm{GHz}}(\mathrm{total}) - 70\mathrm{mJy} \pm 10\mathrm{mJy}\ . \end{aligned}$$

The first two monitoring efforts were with the VLA at 22 GHz in the final quarters of 2009 and 2010 (project codes AR699 and AR717). In 2009, the flux density was steady and slightly elevated relative to the long term average. In 2010, the flux density was steady again and slightly suppressed relative to the long term average. The third monitoring campaign utilized the EVLA at 22 GHz (VLA11B-019) and was executed between October 2011 and January 2012. We detected the decay of what must have been a very strong flare earlier in 2011. In the last quarter of 2012, we switched to AMI for monitoring which is continuing. The advantage of AMI is that it can provide more frequent monitoring with a lower calibration overhead than the EVLA. The disadvantage is that the maximum available frequency is only 18 GHz, (total useful frequency range 13.5 – 18 GHz).

Figure 2 shows the 15.3 GHz light curve from the 8 months of monitoring with AMI. The observations began with the AMI Large Array. However, we noticed flux density variations

that exceeded the formal error estimates from the AMI pipeline but seemed unlikely to be due to source variability. In order to test this hypothesis we began taking simultaneous measurements with the Small Array. The Small Array data appeared much more consistent. We conjecture that the Large Array variations were associated with a high sensitivity to weather conditions which could not be properly calibrated. After realizing this, we switched to only Small Array monitoring. Considering the magnitude of the flare, the accuracy of the Large Array data is adequate as a whole for finding the start of the flare, although any measurement taken individually would be suspect. This is verified by taking the linear fit to the Small Array data near the overlap region and extending it to earlier times in the bottom frame of Figure 2. The flare start is approximately MJD 56185 – 56190.

We only show the AMI data at one frequency in Figure 2 for the sake of clarity since the spectrum is flat and the data points overlap. Typically the spectral index is about $\alpha = 0.1 - 0.2$. However, the data are formally consistent with $\alpha = 0$. The flare in Figure 2 seems to have a magnitude and decay time similar to that indicated by the declining flux density seen in our EVLA observations in the last quarter of 2011 (see Figure 1). The magnitude of this flare is larger than the highest previously measured flux density, $235 \pm 28$ mJy in 1976 at 22.2 GHz (McCutcheon and Gregory 1978). On MJD 56363, the 17.6 GHz flux density was $267 \pm 4$ mJy with a spectral index $\alpha \approx 0.07$, the corresponding spectral energy, was $\nu L_\nu = 1.9 \times 10^{41}$ergs/s.

## 4. Comparison to Blazar Flares

Given the blazar-like properties of Mrk 231 noted in Section 2, we compare the strong flare in the 17.6 GHz light curve from AMI to archival 22 GHz blazar flare light curves in this section. Large blazar flares are typically associated with the ejection of components from the nucleus that can be detected on parsec scales with VLBI. Famous examples include 3C 273 and BL Lacertae (Abraham et al. 1996; Krichbaum et al. 1990; Mutel et al. 1990; Tateyama et al. 1999). However, counter-examples exist when the core brightens, yet no ejected component is resolved with VLBI (Savolainen et al. 2002). We pick the frequency of 22 GHz since it is high enough that the total flux density will be dominated by the flat spectrum radio core. Furthermore, a large data set at 22 GHz of blazar light curves can be found in Teräsranta et al. (2004).

### 4.1. Flare Definition

We define a flare as *an abrupt change in a light curve that results in a dramatic increase above the quiescent background that precedes the flare.* There are two quantitative components to describe this behavior: the abrupt change that is expressed in terms of the time rate of increase of the light curve, $\dot{S}$, and the large local maximum of the light curve, $P$. These parametric descriptions are best expressed in units that are normalized to the quiescent flux density level, $Q$, that precedes the flare, i.e., the normalized amplitude $P/Q$ and $\dot{S} = (P/Q)/(\text{flare rise time})$. The reason for the normalization is the following. Consider a source with a quiescent flux density of $Q \sim 100$ mJy. A $\sim 100$ mJy increase in flux density is a very significant relative change, $P/Q \approx 2$. By contrast if the quiescent flux density is $Q \sim 5$ Jy, $\sim 100$ mJy increase in flux density is imperceptible, $P/Q \approx 1.02$. A second critical aspect of defining a peak in the flux density is that the local maximum be statistically significant above the noise level of the quiescent background. This is important since high frequency survey observations can have significant uncertainty if the flux density is modest (Teräsranta et al. 2004). The standard that we adopt for defining a local maximum corresponding to a flare peak in the light curve is that the putative peak is $P - Q > 3\sigma_{\rm total}$ above the quiescent baseline level, where $\sigma_{\rm total}$ combines the uncertainty in the baseline and peak measurements in quadrature, $\sigma^2_{\rm total} = \sigma^2_{\rm baseline} + \sigma^2_{\rm peak}$.

### 4.2. Defining the Quiescent Baseline

A key element for defining the flare is the determination of quiescent flux density that precedes the putative flare. This can be difficult in general due to source flickering that is on the same order of magnitude as the statistical uncertainty in each measurement and occasionally a second flare occurs during the rise of a previously initiated flare. Generally, in the latter circumstance, these flares are not considered in our statistical analysis since there is so much uncertainty created by this circumstance. The only exception is if the second flare is clearly much weaker than the first flare (i.e., it is essentially large flicker noise). Our working definition of the baseline is a minimum of 4 consecutive observations which agree within the $1\sigma$ uncertainty and do not show a trend of increasing in time. This data is linearly fit to determine the local (in time) baseline quiescent level.

### 4.3. The Radio Flares of Mrk 231 in the Context of Blazars

We compare the flare in Mrk 231 to those of the flares discovered by long term monitoring of $\sim 200$ flat spectrum radio sources at 22 GHz (Teräsranta et al. 2004). We compare the flares in the 22 GHz light curves to the flares in Mrk 231. Due to the condition defining a statically significant flare, $P - Q > 3\sigma_{\rm total}$, all flares satisfy $P/Q > 1.2$. Thus, we effectively segregate traditional blazars from other less violently variable flat spectrum AGN (non-blazars are rare in this high frequency selected sample). The other implication of the $P-Q > 3\sigma_{\rm total}$ condition is that for noisy light curves, many flares cannot be discerned cleanly from the noise using this standard and are excluded from our analysis. A second complicating feature are gaps in the temporal coverage that do not allow one of the following three quantities to be determined, $Q$, $P$ or the start of the flare. Other flares are excluded from our analysis due to a poor determination of $Q$ that arises not only from gaps in sampling, but noise superimposed on low flux density levels or uncertainty due to two or more compound flares. In the end, we found 106 suitable flares in Teräsranta et al. (2004). The distribution of $\dot{S}$ and $P/Q$ is plotted in Figure 3. In order to compare $\dot{S}$ of objects at different redshifts, the data were converted into the elapsed time as measured in the QSO rest frame. The comparison of $\dot{S}$ and $P/Q$ from the blazar sample and the Mrk 231 flare shows that the 2013 flare is in-family (rise time and relative magnitude) with blazar flares. If we consider the background contributions from Equation 1, $S_{\nu=22{\rm GHz}}({\rm core})$ tripled in 2013, from $\approx 65$ mJy to $\approx 195$ mJy in $\sim 150$ days. Based on two observations with VLBA, we can get crude estimates of the parameters for the 2006 flare in Figure 1, $P/Q \sim 1.42$, $\dot{S} \sim 0.48$/month, also in-family with the blazar flares in Figure 3.

## 5. Conclusion

In this letter, we demonstrated that strong,blazar-like, flares were detected in the radio quiet quasar, Mrk 231. Furthermore, this is occurring in a BALQSO in which the radio jets are typically suppressed. Ostensibly, Mrk 231 is on the verge of becoming radio loud, but the relativistic energy stream from the central engine is being stifled by the BAL wind.

Another example of a strong radio flare in a radio quiet quasar is III Zw 2. The magnitude of the flare in 1999 in this object is much more extreme. The 22 GHz flux increases by a factor of $\sim$15 in 1.8 years (Teräsranta et al. 2004). The amplitude is off the chart in the top frame of Figure 3 and $\dot{S} = 0.69$/month is also larger than the 2013 flare for Mrk 231. Such extreme behavior occurs preferentially in radio quiet quasars since $Q$ is generally small and the occasional large flare will be amplified by this normalization. For example, the 1976 flare at 22.2 GHz in Mrk 231 discussed in Reynolds et al. (2009), is very

abrupt. It increased by $134 \pm 37.5$ mJy in 0.033 months, which leads to a relatively large $P/Q = 2.33 \pm 0.65$ and an extremely large value of $\dot{S} = 70 \pm 20$/month, which is off the chart in the bottom frame of Figure 3. In spite of such dramatic behavior in these radio quiet quasars there is one benign property of these flares that indicates the radio quietness. The increase in the intrinsic radio flux density of the flare (in the QSO rest frame) is very low compared to the much higher redshift blazars in Teräsranta et al. (2004). Thus, the variability brightness temperatures for the 2013 Mrk 231 and the 1999 III Zw 2 flares are modest, $3.3 \times 10^{10}$ K and $5.4 \times 10^{10}$ K, respectively, per the methods of Ghosh and Punsly (2007), $\sim 3$ orders of magnitude less than strong blazar flares.

In conclusion, blazar-like flares are not rare in Mrk 231, we detect one in various stages of evolution half the time that we observe the source. Further comparison to blazar flares can be made if superluminal ejections are detected with VLBI observations that are triggered by a flare detected with AMI monitoring. We currently have approved VLBA observations to pursue this.

## 6. Acknowledgments

The National Radio Astronomy Observatory is a facility of the National Science Foundation operated under cooperative agreement by Associated Universities, Inc. This work made use of the Swinburne University of Technology software correlator, developed as part of the Australian Major National Research Facilities Programme and operated under licence. This research has made use of NASA's Astrophysics Data System Bibliographic Services.

## REFERENCES

Abraham, Z., Carrara, E., Zensus, A. and Unwin, S. 1996, A&A, 115, 543

Becker., R. et al. 2000, ApJ, 538, 72

Becker., R. et al. 2000, ApJS, 135, 227

Blundell, K., Beasley, A., Bicknell, G. 2003, ApJL, 591, 103

Briggs, F. H., Turnsheck, D. A., Wolfe, M. 1984, ApJ, 287, 549

Bruni, G. et al. 2013 A&A in press http://xxx.lanl.gov/abs/1304.3021

Brunthaler, A. et al. 2000, A&A, 357, L45

Edelson, R., 1987, ApJ, 313, 651

Ghosh, K. and Punsly, B. 2007, ApJL, 661, 139

Gibson, R. et al. 2009, ApJ, 692, 758

Hayashi, T., Doi, A., Nagai, H. 2013 to appear in ApJ http://xxx.lanl.gov/abs/1305.3371

Hewett, P. and Foltz, C., 2003, AJ, 125, 1784

Krichbaum, T. 1990, A&A, 237, 3

Kettenis, M. et al. 2006, Astron. Data Anal. Software Syst. XV, 351, 497

Marscher, A. et al. 1979, ApJ, 233, 498

McCutcheon, W., Gregory, P. 1978, AJ, 83, 566

Mutel, R. et al., Phillips, R., Su, B., Bucciferro, R. 1990, ApJ, 352, 81

Punsly, B. 2006, ApJ, 647, 886

Reynolds, C., Punsly, B. Kharb, P., O'Dea, C. and Wrobel, J. 2009, ApJ, 706, 851

Savolainen, T., Wiik, K., Valtaoja, E., Jorstad, S., Marscher, A. 2002, A&A, 394, 851

Shepherd, M., Pearson, T., Taylor, G. 1994, BAAS, 27, 903

Tateyama, C. et al. 1999, ApJ, 520, 627

Teräsranta, H. et al. 2004, A&A, 427, 769

Ulvestad, J., Wrobel, J. and Carilli, C. 1999, ApJ, 516, 134

Ulvestad, J. et al. 1999, ApJL, 517, L81

Weymann, R.J., Morris, S.L., Foltz, C.B., Hewett, P.C. 1991, ApJ, 373, 23

Weymann, R. 1997 in ASP Conf. Ser. 128, Mass Ejection from Active Nuclei ed, N.Arav, I. Shlosman and R.J. Weymann (San Francisco: ASP), 3

Zhang, S. et al. 2010, ApJ, 714, 367

Zwart, J. et al. 2008, MNRAS, 391, 1545

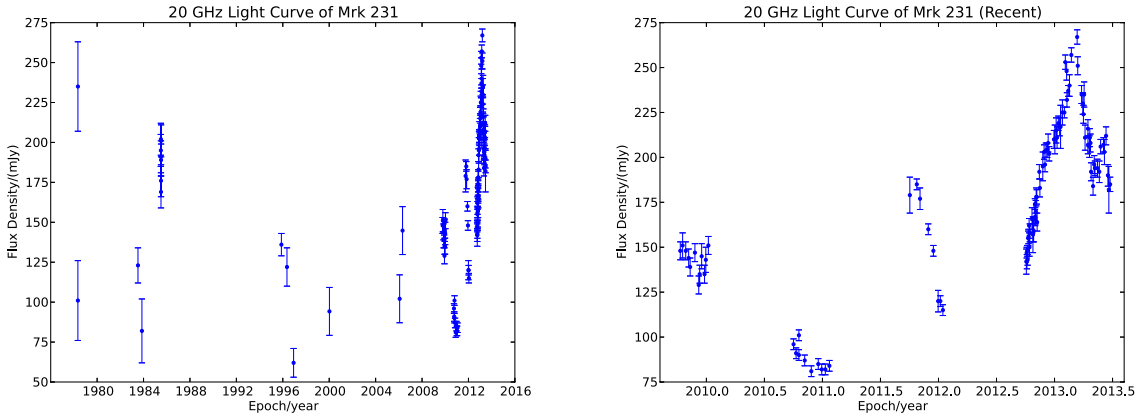


Fig. 1.— The left panel shows the long term, 35 year, light curve at $\sim$ 20 GHz. The right hand panel is a zoom in on the more recent data, with its much more frequent sampling.

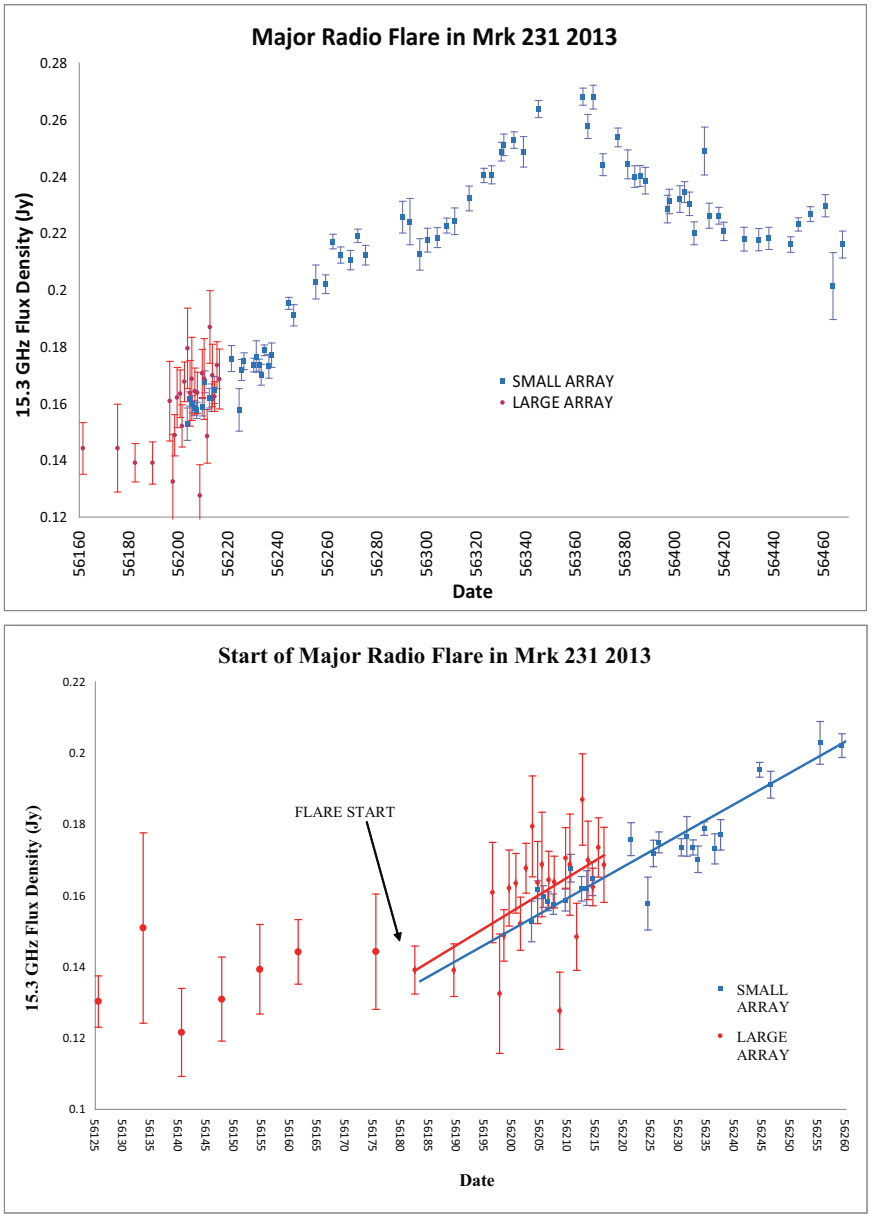


Fig. 2.— The top panel of the figure shows the AMI light curve at 15.3 GHz (a traditional AGN monitoring frequency). The similar flux density levels to those of the 17.6 GHz light curve in Figure 1 is indicative of the fact that the spectrum was flat at most epochs. The light curve includes both AMI-LA data and SA data. The close-up view in the bottom frame is used to estimate the beginning of the flare. Notice that in spite of the systematic errors in the LA data, the linear fit to the data (the red line) yields almost the same start time as the linear fit to the SA data (the blue line). The $\sim 0-2$ day difference is insignificant compared to the $\sim 150$ day rise time of the flare.

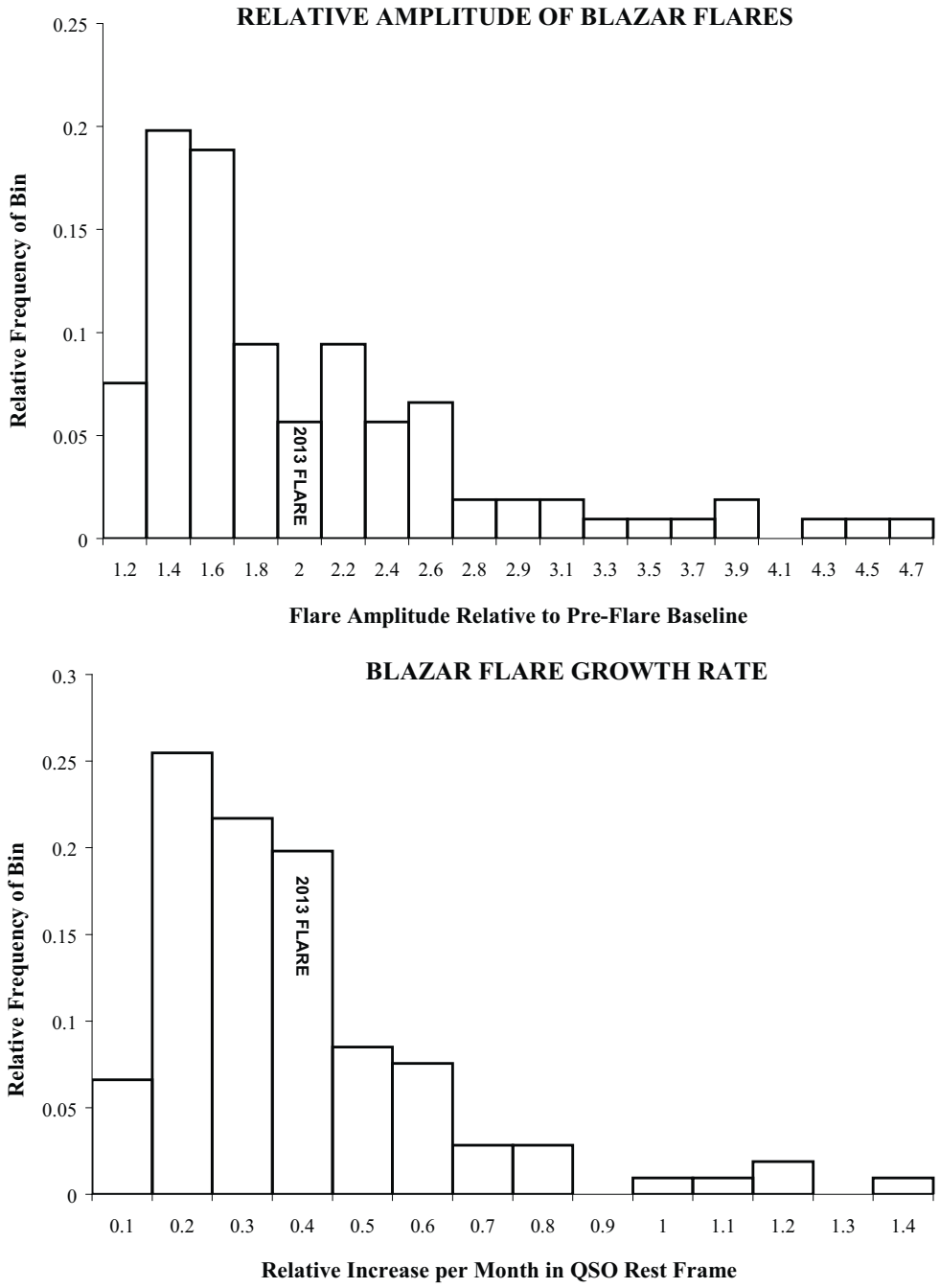


Fig. 3.— Comparison of the 2013 flare in the Mrk 231 to the distribution of flare parameters in the Teräsranta et al. (2004) blazar sample. The top frame shows the distribution of the normalized flare amplitude, $P/Q$. The bottom frame is the time rate of increase in normalized units, $\dot{S} = (P/Q)/(\text{rise time})$, from the quiescent baseline to the flare peak (units are months$^{-1}$). Two flares from Teräsranta et al. (2004) are very abrupt and are off the bottom histogram, to the right.